



# Self-healing of a heralded single-photon Airy beam

ZHI-XIANG LI,<sup>1</sup> YA-PING RUAN,<sup>1</sup> JIE TANG,<sup>2</sup> YUAN LIU,<sup>1</sup> JIAN-JI LIU,<sup>3</sup> JIANG-SHAN TANG,<sup>1</sup> HAN ZHANG,<sup>1</sup> KE-YU XIA,<sup>1,4</sup>  AND YAN-QING LU<sup>1,5</sup>

<sup>1</sup>National Laboratory of Solid State Microstructures, College of Engineering and Applied Sciences, and Collaborative Innovation Center of Advanced Microstructures, Nanjing University, Nanjing 210093, China

<sup>2</sup>School of Science, Nantong University, Nantong 226019, China

<sup>3</sup>The MOE Key Laboratory of Weak-Light Nonlinear Photonics, School of Physics and TEDA Applied Physics Institute, Nankai University, Tianjin 300457, China

<sup>4</sup>keyu.xia@nju.edu.cn

<sup>5</sup>yqlu@nju.edu.cn

**Abstract:** Self-healing of an Airy beam during propagation is of fundamental interest and also promises important applications. Despite many studies of Airy beams in the quantum regime, it is unclear whether an Airy beam only including a single photon can heal after passing an obstacle because the photon may be blocked. Here we experimentally observe self-healing of a heralded single-photon Airy beam. Our observation implies that an Airy wave packet is robust against obstacle caused distortion and can restore even at the single-photon level.

© 2021 Optical Society of America under the terms of the [OSA Open Access Publishing Agreement](#)

## 1. Introduction

The Airy wave packet was first predicted in the context of quantum mechanics: a free particle can exhibit a non-spreading Airy wave packet solution, as a result of interference effects following proper preparation of the initial Schrödinger wave function [1]. An ideal Airy wave packet is accompanied by infinite energy. Such property hinders the experimental realization of an ideal Airy beam. More than two decades later, a quasi-diffraction-free Airy wave packet with finite energy was proposed by Siviloglou [2,3]. Since then, the unique properties of Airy beams including propagation-invariant, self-bending, and self-healing have attracted considerable research interests [4,5]. Moreover, Airy beams in combination with other structured light, such as vortex Airy beams (VABs) carrying orbital angular momentum, have been widely investigated for high-dimensional information processing [6–12].

Recently, quantum Airy beams have attracted great attention. Quantum polarization fluctuations of an Airy beam in turbulent atmosphere has been theoretically investigated in a slant turbulent channel [13]. Their results indicate that Airy beams have potential for important applications in long-distance free-space quantum communication system. An Airy beam generated from spontaneous parametric down-conversion (SPDC) process has demonstrated the maintenance of quantum correlation during the parabolic propagation in the quantum domain [14]. Spatially entangled Airy beam has also been reported [15]. However, to the best of our knowledge, the self-healing property of Airy beams in the quantum domain is yet to observe.

Self-healing is the ability of a light beam to reconstruct after propagation through an obstacle. It is firstly studied in coherent diffraction-free beams, such as Bessel beams [16], Airy beams [17], caustic beams [18], Mathieu and Weber beams [19]. Later, the self-healing ability of diffracting coherent beams have been pursued, including vector Laguerre–Gaussian beams [20], radially polarized [21] and tightly focused [22] Bessel–Gauss beams, and Pearcey beams [23], etc. Moreover, the self-healing of partially coherence beams has also attracted much attention [24–28]. The self-healing property has been explained with the theory of a classical field through

internal transverse power flow analysis [17,29], Babinet's principle [16], or ray tracing pictures [30,31]. This characteristic is of particular importance for an Airy beam during light propagation in inhomogeneous media. It also proved to be important in the field of microscopy [32,33] and has been used to improve image quality in a ghost imaging system [34]. Here we consider the self-healing property of Airy beams. Can single photon Airy beam recovery after propagating through an obstruction as a classical Airy beam does?

In this paper, for the first time, we report experimental observation of self-healing of a two-dimensional single-photon Airy beam generated from a heralded single-photon source. Our observation shows that the Airy beam can heal after distortion caused by an obstacle at the single-photon level. Considering that double-slit interference of single photons reveals many fundamental features of quantum mechanics, self-healing ability of an Airy wave packet at single-photon level may shed light to interpretation of quantum feature of a single photon essentially different from which path question.

## 2. Methods and experiments

In our experiment, heralded single photons are produced from SPDC process. We use a 10-mm-long PPKTP crystal (Raicol Crystals) with a grating period of 10  $\mu\text{m}$  for frequency-degenerate type-II quasi-phase matched collinear SPDC. The experimental setup to generate photon pairs is depicted in Fig. 1(a). We use a continuous-wave diode laser at 405 nm as the pump laser. The maximum laser power is 24 mW. Polarization entangled photons are generated via the SPDC process based on a Sagnac interferometer scheme [35]. The crystal is antireflection coated at 405 nm and 810 nm. The temperature of PPKTP is set at 27.8°C with the stability of  $\pm 0.1^\circ\text{C}$  by a heating oven. The PSI consisted of two flat mirrors, a dual-wavelength half-wave plate (DHWP), and a dual-wavelength PBS (DPBS). The DHWP and DPBS work well at both pump and output wavelengths. The generated SPDC photon pairs are collimated by a lens with a focal length of 200 mm. The 10 nm narrow bandwidth interference filters (IFs) centered at a wavelength of 810 nm are used to block the resident pump laser. The polarization states of the signal and idler photons are analyzed with a combination of an HWP and a polarizer before detection by single-photon counting modules (SPCM, Perkin-Elmer SPCM-AQR-14). The output quantum state is set as  $|H_s\rangle|V_i\rangle + |V_s\rangle|H_i\rangle$  by tuning the input polarization [35]. The coincidence count of the photon pair is 90000 per second measured with a coincidence measurement time window  $\Delta t_c = 5$  ns. Figure 1(b) shows the measured normalized coincidences as a function of the polarization analyzer angle when the idler polarization analyzer angle fixed at  $0^\circ$  and  $45^\circ$ .

We then use the photon pairs to generate heralded single photons. To characterize the heralded single-photon source, we measure the conditional second-order coherence function, which is defined as the second-order correlation for the signal field conditioned on successfully detecting an idler photocount [36,37]:

$$g_c^{(2)}(t_1, t_2 | t_i) \equiv \frac{\langle \hat{E}_s^\dagger(t_1) \hat{E}_s^\dagger(t_2) \hat{E}_s(t_2) \hat{E}_s(t_1) \rangle_{\text{pm}}}{\langle \hat{E}_s^\dagger(t_1) \hat{E}_s(t_1) \rangle_{\text{pm}} \langle \hat{E}_s^\dagger(t_2) \hat{E}_s(t_2) \rangle_{\text{pm}}} \quad (1)$$

where  $\langle \dots \rangle_{\text{pm}}$  is the ensemble average over the post-measurement states. We experimentally tested the special case of  $g_c^{(2)}(\tau) \equiv g_c^{(2)}(t_i, t_i + \tau | t_i) = g_c^{(2)}(0, \tau | 0)$ . As shown in the dashed box in Fig. 1(a), the signal beam goes through an Hanbury Brown and Twiss (HBT) interferometer consisting of a 50:50 beam splitter followed by two filters. The detection events between the three channels ( $i$ ,  $s_1$ , and  $s_2$ ) are recorded by a time-correlated single-photon counting device (TCSPCD) operated in the time-tagged mode. The digital resolution of the TCSPC is 64 ps.

The calculated  $g_c^{(2)}(\tau)$  with two different coincidence windows are shown Fig. 1(c). An antibunching feature is clearly visible. The conditional second-order coherence implies the normalized probability of simultaneously observing the signal photons in the  $s_1$  and  $s_2$  paths

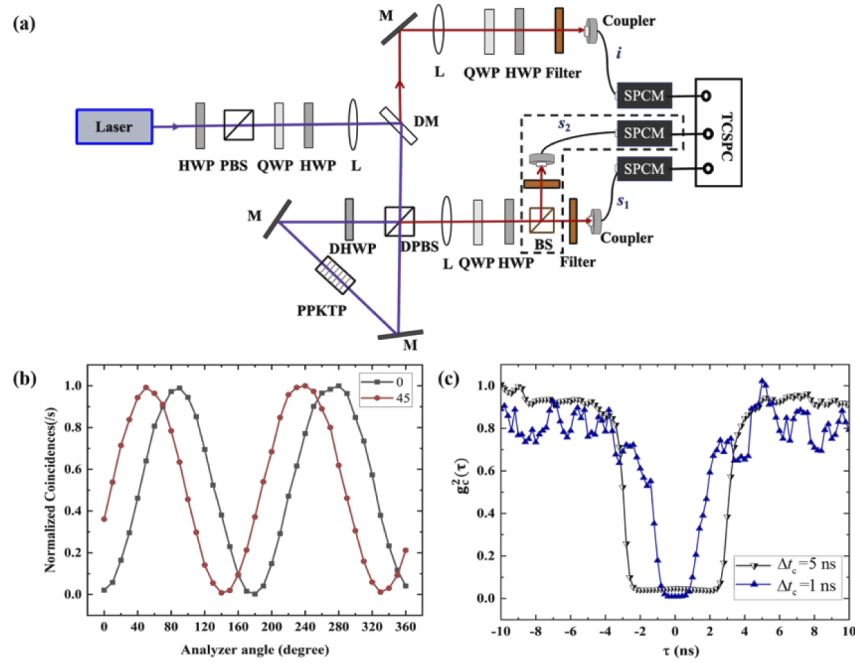


**Fig. 1.** (a) Experimental setup to generate photon pairs via the SPDC process. QWP: quarter-waveplate, HWP: half-waveplate, PBS: polarizing beam splitter, L: Lens, M: mirror, DM: dichroic mirror, DPBS: dual-wavelength PBS, DHWP: dual-wavelength HWP, SPCM: single-photon counting module, TCSPC: time-correlated single-photon counting. (b) Coincidence counts as a function of signal polarization analyzer angle for different settings of idler polarization analyzer angle. (c) Conditional second-order coherence is  $g_c^{(2)}(\tau)$  with 1 ns and 5 ns coincidence window.

within a coincidence measurement time window  $\Delta t_c$ , when the idler photon is detected. Thus, a smaller  $\Delta t_c$  gives a higher temporal resolution of a single-photon property. As a result, a smaller coincidence time window normally generates a deeper but narrower central dip in the conditional second-order coherence measurement. We obtain  $g_c^{(2)}(0) = 0.01$  with  $\Delta t_c = 1$  ns and  $g_c^{(2)}(0) = 0.04$  with  $\Delta t_c = 5$  ns. This small value of  $g_c^{(2)}(0)$  implies that our heralded single-photon source is of good quality and the two- or multi-photon events can be neglected.

We use an experiment setup shown in Fig. 2 to generate the Airy pattern including a heralded single photon. The signal beam generated from the SPDC process is coupled out from the optical fiber by a second fiber-port and then passes through a polarizing beam splitter. Later the photons are incident on a reflective spatial light modulator (SLM) with the desired cubic phase modulation PM, generating an Airy pattern at the focal plane of the lens L. The SLM has  $1920 \times 1080$  pixels with pixel pitch of  $8 \mu\text{m}/\text{pixel}$ .

The optical elements are aligned by using a reference fiber laser working at a wavelength near 810 nm. The generated Airy pattern using the reference laser is shown in Fig. 3(a). The beam pattern is magnified by 4 times and imaged with an imaging lens (not shown here). The image is obtained by intensified CCD (iCCD) working at  $-30^\circ\text{C}$ , with an exposure time of  $\Delta t_e = 1$  s. The intensity distribution of the Airy wave packet is given by [38]

$$I(x, y) = \left| \text{Ai}\left(\frac{x}{x_0}\right) \right|^2 \exp\left(2\frac{\alpha x}{x_0}\right) \left| \text{Ai}\left(\frac{y}{y_0}\right) \right|^2 \exp\left(2\frac{\alpha y}{y_0}\right) \quad (2)$$

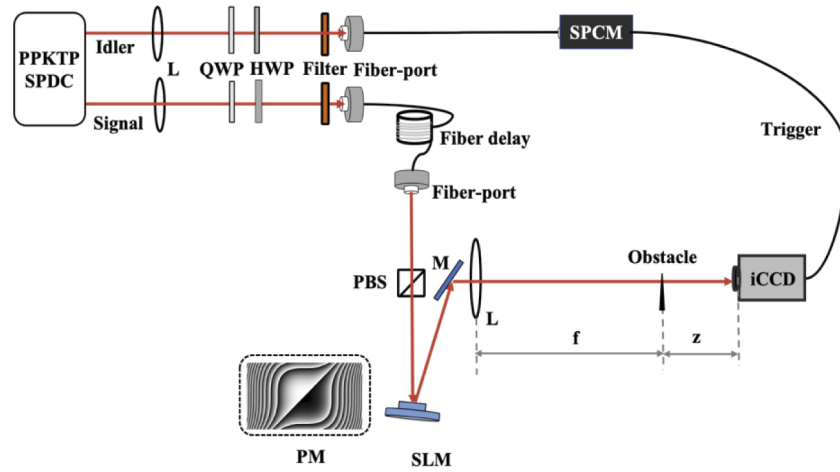


**Fig. 2.** Experimental setup for self-healing observation of an Airy beam at the single-photon level. QWP: quarter-waveplate, HWP: half-waveplate, PBS: polarizing beam splitter, M: mirror, SLM: spatial light modulator, PM: phase modulation.

where  $Ai$  represents the Airy function,  $x_0$  and  $y_0$  are the scaling factors in  $x$  and  $y$  transverse directions, respectively, and  $\alpha$  the truncation factor.

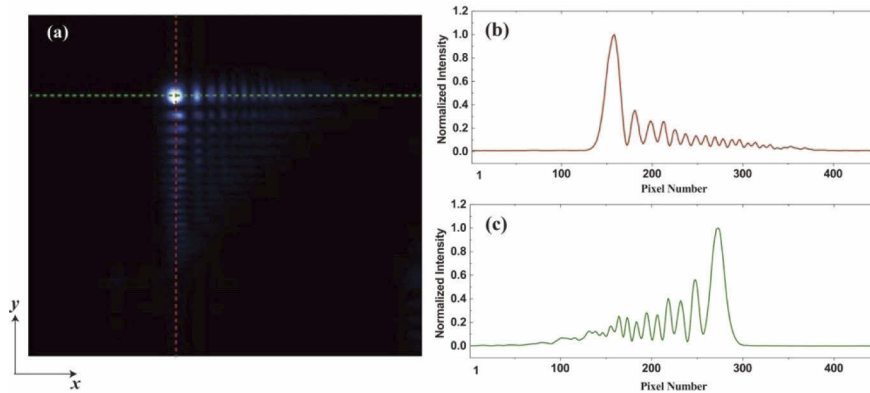


**Fig. 3.** The intensity distribution Airy beam. (a) The 2D intensity distribution of Airy beam; (b) The intensity distribution along  $x$  axis (the red dashed line); (c) The intensity distribution along  $y$  axis (the green dashed line).

The light intensity along the dashed lines of the Airy beam is shown in Figs. 3(b) and 3(c). We can clearly see the central energy distributions of different lobes. The FWHM of the main lobe of the Airy beam is measured to be  $80 \mu\text{m}$ , corresponding to  $x_0 = y_0 \approx 40 \mu\text{m}$  and  $\alpha = 0.1$ .

Then, we test the generation of a single-photon Airy beam. We create heralded single photons with the aforementioned setup shown in Fig. 2. The idler beam is used to trigger the iCCD for detection of signal photons [39–42]. The iCCD triggering mechanism leads to an electronic delay of 70 ns. In our experiment, a 22 m optical fiber delay line is used to compensate for the electric delay of iCCD, ensuring that the signal photons reach the camera at the same time when the camera is triggered by the heralding detector. To measure the data shown in Fig. 4, we set the coincidence gate time window to 5 ns which is a commonly used parameter for single photon imaging experiments [39]. The available time window is limited by our iCCD. The small value of

$g_c^{(2)}(0) = 0.04$  with  $\Delta t_c = 5$  ns implies that our heralded photon source can generate single photons with a high purity. During  $\Delta t_c$ , to a good approximation, there is at most one photon reaching the detection plane of iCCD. The iCCD is in the integrate-on-chip mode with an exposure time  $\Delta t_e = 0.5$  s. The exposure time  $\Delta t_e$  determines the accumulating period of the signal photons on the chip before the imaging is readout.

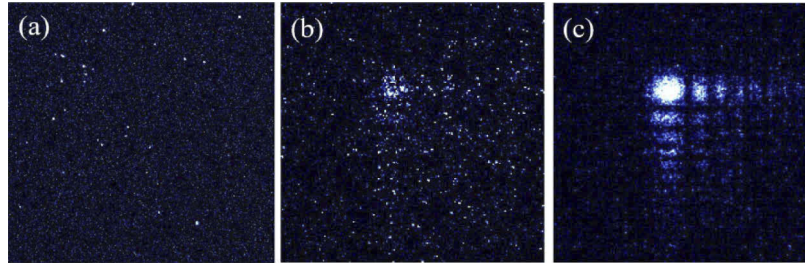


**Fig. 4.** Experimentally observation of forming an Airy beam at the single-photon level. The distribution of Airy wave-packet with (a) one frame, (b) 50 frames and (c) 500 frames, with each frame contains 3500 accumulations of single-photon events.

When only one frame is considered, the image pattern cannot form because there are not enough detected photons to display the image. As single-photon behavior is probabilistic, measuring a quantum state doesn't produce the same outcome every time. By accumulating many outcomes that each occur with a certain probability, the single photon Airy beam distribution can be obtained. Figure 4(a) shows a single frame that records the intensity distribution with an exposure time of 0.5 s. The random bright spots show no pattern. Figures 4(b) and 4(c) show the image accumulating for  $N=50$  and 500 frames, respectively. As the accumulated frame number  $N$  increases, the Airy pattern gradually becomes clearer.

Note that the intensity distribution of Airy pattern shown in Fig. 4(c) is the accumulation of over one million photon events. The heralded single photons are generated at a rate of 90 kHz. The overall transmission efficiency as the photons go through the experimental setup is 39% and the quantum efficiency of the iCCD at wavelength of 810 nm is 20%. Thus, the photons are detected by the iCCD at a rate of 7 kHz. As each frame is set to be 0.5 s, for observation of Fig. 4(c), there is totally 1.75 million photon events involved.

To demonstrate the self-healing properties of a single-photon Airy beam, we block the main lobe of the single-photon Airy beam by using an opaque obstacle and then monitor their self-healing during propagation. The photons generated from our single-photon source reach the SLM and the iCCD one by one within a time resolution, finally accumulating to the images shown in Fig. 5.

The reconstruction process of the Airy profile is shown in Fig. 5. We can see the blocked intensity distribution at  $z = 0$  in Fig. 5(a). The intensity distributions of the signal field beam after propagating a distance of 5 mm and 10 mm are shown in Figs. 5(b) and 5(c), respectively. It can be seen that a full Airy beam can heal at position 10 mm. Our results confirm that the self-healing of an Airy beam is robust against distortion caused by an obstacle even at the single-photon level. The self-healing effect of single-photon Airy beam reflects the wave-particle duality of a single-photon light beam. This single-photon Airy beam exhibits the wave property during propagation and thus can restore as a coherent Airy beam. However, when it is detected, it appears as discrete particle. Therefore, the single-photon Airy beam creates a single bright dot on iCCD each time.

The physics behind the self-healing of a single-photon Airy can be explained through Born's statistical interpretation of the wave function. The probability of finding a photon at a given position is proportional to the square of Airy wave function amplitude, i.e., the intensity of the



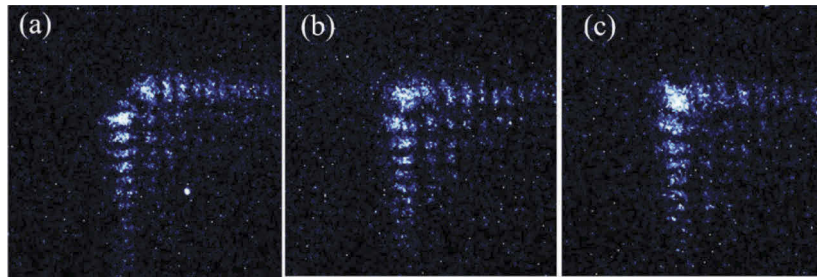


**Fig. 5.** Self-healing of Airy beam when the main lobe is blocked. The observed intensity profiles at (a) the input plane  $z = 0$ , (b)  $z = 5$  mm and (c)  $z = 10$  mm. The images are accumulated by 500 frames. Each frame contains 3500 accumulations of single-photon events.

Airy beam. When an obstacle is placed to block the main lobe, a photon can either be lost or preserved with the corresponding probability. After passing a certain distance, the main lobe is recovered as a result of photon interference. Only through accumulating many single-photon events, the Airy beam intensity distribution can be observed.

### 3. Summary

We have experimentally observed self-healing of a heralded single-photon Airy beam. When the main lobe is blocked by an obstacle, the single-photon Airy beam still has the capability of reconstructing its pattern after propagating a certain distance. Our work shows the potential of using Airy beams to improve quantum communications. In combination with structured light, our study of Airy beams in the quantum domain may provide new opportunities for distortion-immune high-dimensional quantum information processing.

**Funding.** National Key Research and Development Program of China (2017YFA0303700, 2019YFA0308700); National Natural Science Foundation of China (11690031, 11874212, 11890704, 12004200, 12104242); Natural Science Foundation of Jiangsu Province (BK20212004); Program for Innovative Talents and Entrepreneurs in Jiangsu.

**Acknowledgement.** We thank Prof. Lijiang Zhang and Prof. Yi Hu for technical support with the experiment and helpful discussions.

**Disclosures.** The authors declare no conflicts of interest.

**Data availability.** Data underlying the results presented in this paper are not publicly available at this time but may be obtained from the authors upon reasonable request.

### References

1. M. V. Berry and N. L. Balazs, "Nonspreading wave packets," *Am. J. Phys.* **47**(3), 264–267 (1979).
2. G. A. Siviloglou and D. N. Christodoulides, "Accelerating finite energy Airy beams," *Opt. Lett.* **32**(8), 979 (2007).
3. G. A. Siviloglou, J. Broky, A. Dogariu, and D. N. Christodoulides, "Observation of Accelerating Airy Beams," *Phys. Rev. Lett.* **99**(21), 213901 (2007).
4. N. K. Efremidis, Z. Chen, M. Segev, and D. N. Christodoulides, "Airy beams and accelerating waves: an overview of recent advances," *Optica* **6**(5), 686 (2019).
5. Y. Hu, G. A. Siviloglou, P. Zhang, N. K. Efremidis, D. N. Christodoulides, and Z. Chen, "Self-accelerating Airy Beams: Generation, Control, and Applications," in *Nonlinear Photonics and Novel Optical Phenomena*, Z. Chen and R. Morandotti, eds. (Springer, New York, 2012), pp. 1–46.
6. H. L. I. Ui, H. A. L. Iu, and X. I. C. Hen, "Nonlinear generation of Airy vortex beam," *Opt. Express* **26**(16), 21204–21209 (2018).
7. B.-Y. Wei, S. Liu, P. Chen, S.-X. Qi, Y. Zhang, W. Hu, Y.-Q. Lu, and J.-L. Zhao, "Vortex Airy beams directly generated via liquid crystal q-Airy-plates," *Appl. Phys. Lett.* **112**(12), 121101 (2018).
8. Y. Liu, W. Chen, J. Tang, X. Xu, P. Chen, C.-Q. Ma, W. Zhang, B.-Y. Wei, Y. Ming, G.-X. Cui, Y. Zhang, W. Hu, and Y.-Q. Lu, "Switchable Second-Harmonic Generation of Airy Beam and Airy Vortex Beam," *Adv. Opt. Mater.* **9**(4), 2001776 (2021).
9. Z.-X. Fang, Y. Chen, Y.-X. Ren, L. Gong, R.-D. Lu, A.-Q. Zhang, H.-Z. Zhao, and P. Wang, "Interplay between topological phase and self-acceleration in a vortex symmetric Airy beam," *Opt. Express* **26**(6), 7324 (2018).

10. R.-P. Chen and C. H. R. Ooi, "Nonclassicality of vortex Airy beams in the Wigner representation," *Phys. Rev. A* **84**(4), 043846 (2011).
11. X. Peng, Y. Peng, D. Li, L. Zhang, J. Zhuang, F. Zhao, X. Chen, X. Yang, and D. Deng, "Spatiotemporal controllable Airy–Airy-vortex light bullets in free space," *Laser Phys. Lett.* **14**(12), 126001 (2017).
12. Q. Yang, Y. Gong, Z. Huang, Z. Luo, H. Li, and D. Deng, "Propagation properties of the radially polarized Airy vortex beams in a chiral medium," *Appl. Opt.* **59**(9), 2849 (2020).
13. X. Yin and L. Zhang, "Quantum polarization fluctuations of an Airy beam in turbulent atmosphere in a slant path," *J. Opt. Soc. Am. A* **33**(7), 1348 (2016).
14. S. Maruca, S. Kumar, Y. M. Sua, J.-Y. Chen, A. Shahverdi, and Y.-P. Huang, "Quantum Airy photons," *J. Phys. B: At. Mol. Opt. Phys.* **51**(17), 175501 (2018).
15. O. Lib and Y. Bromberg, "Spatially entangled Airy photons," *Opt. Lett.* **45**(6), 1399 (2020).
16. Z. Bouchal, J. Wagner, and M. Chlup, "Self-reconstruction of a distorted nondiffracting beam," *Opt. Commun.* **151**(4-6), 207–211 (1998).
17. J. Broky, G. A. Siviloglou, A. Dogariu, and D. N. Christodoulides, "Self-healing properties of optical Airy beams," *Opt. Express* **16**(17), 12880 (2008).
18. M. Anguiano-Morales, A. Martínez, M. D. Iturbe-Castillo, S. Chávez-Cerda, and N. Alcalá-Ochoa, "Self-healing property of a caustic optical beam," *Appl. Opt.* **46**(34), 8284 (2007).
19. P. Zhang, Y. Hu, T. Li, D. Cannan, X. Yin, R. Morandotti, Z. Chen, and X. Zhang, "Nonparaxial Mathieu and Weber Accelerating Beams," *Phys. Rev. Lett.* **109**(19), 193901 (2012).
20. S. Vyas, M. Niwa, Y. Kozawa, and S. Sato, "Diffractive properties of obstructed vector Laguerre–Gaussian beam under tight focusing condition," *J. Opt. Soc. Am. A* **28**(7), 1387 (2011).
21. G. Wu, F. Wang, and Y. Cai, "Generation and self-healing of a radially polarized Bessel-Gauss beam," *Phys. Rev. A* **89**(4), 043807 (2014).
22. S. Vyas, Y. Kozawa, and S. Sato, "Self-healing of tightly focused scalar and vector Bessel–Gauss beams at the focal plane," *J. Opt. Soc. Am. A* **28**(5), 837 (2011).
23. J. D. Ring, J. Lindberg, A. Mourka, M. Mazilu, K. Dholakia, and M. R. Dennis, "Auto-focusing and self-healing of Pearcey beams," *Opt. Express* **20**(17), 18955–18966 (2012).
24. Y. Liang, D. Song, C. Lou, X. Zhang, J. Xu, and Z. Chen, "Generation and propagation of partially spatially incoherent Airy beams," in CLEO: 2013, OSA Technical Digest (online), QM2E.7.
25. Z. Xu, X. Liu, Y. Chen, F. Wang, L. Liu, Y. E. Monfared, S. A. Ponomarenko, Y. Cai, and C. Liang, "Self-healing properties of Hermite-Gaussian correlated Schell-model beams," *Opt. Express* **28**(3), 2828 (2020).
26. G. Wu and X. Pang, "Self-Healing Properties of Partially Coherent Schell-Model Beams," *IEEE Photonics J.* **9**(6), 1–11 (2017).
27. F. Wang, Y. Chen, X. Liu, Y. Cai, and S. A. Ponomarenko, "Self-reconstruction of partially coherent light beams scattered by opaque obstacles," *Opt. Express* **24**(21), 23735 (2016).
28. G. Wu and C. Tao, "Analytical study of the self-reconstruction of a partially coherent Gaussian Schell-model beam," *Opt. Commun.* **424**, 86–90 (2018).
29. X. Chu, G. Zhou, and R. Chen, "Analytical study of the self-healing property of Airy beams," *Phys. Rev. A* **85**(1), 013815 (2012).
30. M. Mazilu, D. J. Stevenson, F. Gunn-Moore, and K. Dholakia, "Light beats the spread: "non-diffracting" beams," *Laser & Photon. Rev.* **4**(4), 529–547 (2010).
31. Y. Kaganovsky and E. Heyman, "Wave analysis of Airy beams," *Opt. Express* **18**(8), 8440 (2010).
32. F. O. Fahrbach, P. Simon, and A. Rohrbach, "Microscopy with self-reconstructing beams," *Nat. Photonics* **4**(11), 780–785 (2010).
33. T. Vettenburg, H. I. C. Dalgarno, J. Nyk, C. Coll-Lladó, D. E. K. Ferrier, T. Čižmár, F. J. Gunn-Moore, and K. Dholakia, "Light-sheet microscopy using an Airy beam," *Nat. Methods* **11**(5), 541–544 (2014).
34. Y. Zhou, G. Wu, Y. Cai, F. Wang, and B. J. Hoenders, "Application of self-healing property of partially coherent beams to ghost imaging," *Appl. Phys. Lett.* **117**(17), 171104 (2020).
35. T. Kim, M. Fiorentino, and F. N. C. Wong, "Phase-stable source of polarization-entangled photons using a polarization Sagnac interferometer," *Phys. Rev. A* **73**(1), 012316 (2006).
36. E. Bocquillon, C. Couteau, M. Razavi, R. Laflamme, and G. Weihs, "Coherence measures for heralded single-photon sources," *Phys. Rev. A* **79**(3), 035801 (2009).
37. D. Höckel, L. Koch, and O. Benson, "Direct measurement of heralded single-photon statistics from a parametric down-conversion source," *Phys. Rev. A* **83**(1), 013802 (2011).
38. J. E. Morris, M. Mazilu, J. Baumgartl, T. Čižmár, and K. Dholakia, "Propagation characteristics of Airy beams: dependence upon spatial coherence and wavelength," *Opt. Express* **17**(15), 13236 (2009).
39. W.-R. Qi, R. Liu, L.-J. Kong, Z.-X. Wang, S.-Y. Huang, C. Tu, Y. Li, and H.-T. Wang, "Double-slit interference of single twisted photons," *Chin. Opt. Lett.* **18**(10), 102601 (2020).
40. R. Fickler, M. Krenn, R. Lapkiewicz, S. Ramelow, and A. Zeilinger, "Real-Time Imaging of Quantum Entanglement," *Sci. Rep.* **3**(1), 1914 (2013).
41. L. Zhang, L. Neves, J. S. Lundeen, and I. A. Walmsley, "A characterization of the single-photon sensitivity of an electron multiplying charge-coupled device," *J. Phys. B: At. Mol. Opt. Phys.* **42**(11), 114011 (2009).
42. P. A. Morris, R. S. Aspden, J. E. C. Bell, R. W. Boyd, and M. J. Padgett, "Imaging with a small number of photons," *Nat. Commun.* **6**(1), 5913 (2015).